

ATTITUDE MODELING OF BIASED-MOMENTUM 3-AXIS STABILIZED SPACE CRAFT HAYABUSA2 IN SUN-TRACKING MOTION

Kosuke Akatsuka⁽¹⁾, Go Ono⁽²⁾, Yuichi Tsuda⁽²⁾ and Junichiro Kawaguchi⁽²⁾

⁽¹⁾*Department of Aeronautics and Astronautics, The University of Tokyo, 7-3-1 Hongo, Bunkyo-ku, Tokyo, 113-8654, Japan,*

+81-50-336-23042, akatsuka.kosuke@ac.jaxa.jp

⁽²⁾*Institute of Space and Aeronautical Science, Japan Aerospace Exploration Agency, 3-1-1 Yoshinodai, Chuo-ku, Sagami-hara, Kanagawa, 252-5210, Japan*

Abstract: *An attitude model for the biased-momentum 3-axis spacecraft “Hayabusa2” under the influence of solar radiation pressure is presented. It is confirmed from “Hayabusa” and “IKAROS” that the angular momentum vector of a spacecraft can track the sun direction automatically in spite of orbital motion. This motion is called sun-tracking motion. Past studies revealed the mechanism of this sun-tracking motion only for a spin-stabilized spacecraft, so this study extends these analyses to biased-momentum 3-axis stabilized spacecraft. Attitude control using sun-tracking motion efficiently increases redundancy and saves fuel consumption. It is shown that the sun-tracking motion of biased-momentum 3-axis stabilized spacecraft is characterized by 9 parameters. Sun-tracking motion is reproduced by numerical simulation using the 9 parameter values from real flight data, and it confirms that analytical model is reasonable and usable for future period of the mission.*

Keywords: *Attitude control, Solar radiation pressure, Spacecraft modeling, Sun-tracking motion, Hayabusa2*

1. Introduction

In interplanetary missions, solar radiation pressure (SRP) is a major disturbance affecting spacecraft[1]. Some missions, however, utilize this SRP disturbance to stabilize the spacecraft attitude. Two typical examples are; the emergency operation of Hayabusa[2,3] and the attitude control demonstration of IKAROS.[4,5]

In these missions, it is confirmed that the angular momentum vector of a spacecraft can track the sun direction automatically with proper settings, in spite of orbital motion. This motion is called sun-tracking motion. (Fig.1 and Fig.2) Working only one reaction wheel along the axis that needs to be pointing to the sun direction, the spacecraft will roughly point towards that direction. By actively using SRP, this improved attitude control system is realized and efficiently increases redundancy and saves spacecraft fuel consumption. In contrast with the fact that past missions have used this technique exclusively for spin-stabilized spacecraft, this paper attempts to extend this sun-tracking technique to a biased-momentum 3-axis stabilized spacecraft, Hayabusa2[6].

SRP torque working on Hayabusa2 is approximately described by 9 parameters and an analytical attitude model is established using them[7]. It is also confirmed that these 9 parameters are related to the spacecraft shape, and that relation is described using a simple solar sail model, which can easily show the characteristics of shape. Attitude motion is mainly dependent on 6 parameters and the change of inner angular momentum is mainly decided by the other 3

parameters. Analytical attitude motion is a combination phenomenon of precession, torque-induced main attitude motion, and nutation, torque-free circular motion around the angular momentum vector. Interestingly, the equilibrium direction of precession is not exactly the sun direction and the history of precession draws an ellipse. The equilibrium direction has certain offset from the exact sun direction and it depends on the shape of spacecraft and its rotational angle. The ellipse may converge or diverge depending on attitude conditions. These new phenomenon are unique to 3-axis stabilized spacecraft and not observed in spinning spacecraft.

The 9 parameter values are obtained from real flight data of Hayabusa2, using a least-square method. It becomes possible to estimate attitude motion using these 9 parameters. The result of numerical simulation is compared with the real spacecraft behavior and it agrees well with the flight data. The analytical model of sun-tracking motion is proven to be true and this newly derived model is sufficiently effective for prediction of future attitude motion of Hayabusa2.

Attitude motion of a biased-momentum 3-axis stabilized spacecraft is established analytically in this study and it is proven to be true in comparison with flight data. This analytical model is not restricted to Hayabusa2 but is applicable to various 3-axis stabilized spacecraft. Furthermore, this control method is so simple and does not need any new algorithm that sun-tracking motion can be applied to various interplanetary missions in the future.

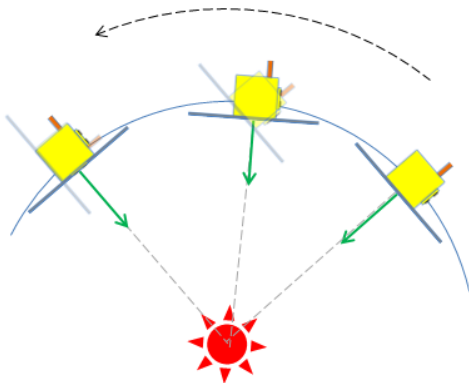


Figure 1. Sun-tracking motion image

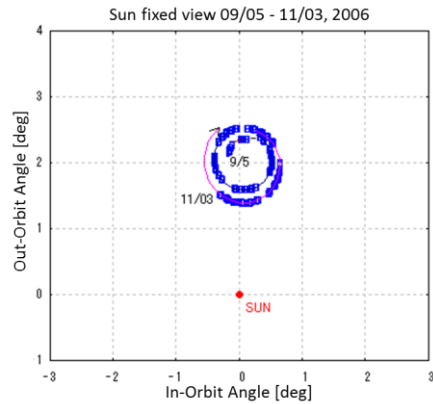


Figure 2. Attitude history of emergency operation of Hayabusa

2. Sun-Tracking Motion

Sun-tracking motion is roughly the same mechanism as the motion of spinning top. Both motions are the combination of precession and nutation. Precession is a torque-induced motion of the angular momentum vector, whereas nutation is a torque-free circular motion of the rotation axis around the angular momentum vector. The precession motion of a spinning top is induced by gravity torque. In the case of a spinning or biased-momentum spacecraft, in interplanetary missions, it is induced by the SRP torque. Precession is described by Euler equation:

$$\left. \frac{d\mathbf{H}}{dt} \right|_I = \mathbf{T} \quad (1)$$

where \mathbf{H} is the angular momentum vector, \mathbf{T} is the external torque vector and subscript I represents the inertial frame observing. This equation says that the angular momentum vector is inclined to the external torque vector direction. The gravity torque field on the spinning top draws a circle around the vertical vector on the ground, and the SPR torque field also draws a circle around the sun direction. In result, the angular momentum vector also draws a circle around the sun direction automatically; this motion is the, so called, sun-tracking motion.

In addition, in the case of an orbiting spacecraft, inertia torque generated by orbital motion affects the spacecraft. Because of that, the center of sun-tracking motion, which is the equilibrium point where total torque is zero, is shifted in the out-orbit direction. In result, the angular momentum vector of the spacecraft draws a circle around that shifted equilibrium point. This phenomenon is common to spinning spacecraft and biased-momentum spacecraft.

This study reveals that only in the case of biased-momentum 3-axis stabilized spacecraft, the equilibrium point is shifted not only in the out-orbit direction, but also in the in-orbit direction, and that the precession motion is not necessarily a perfect circle, it would be elliptic and diverge or converge. It is because the additional SRP is working on biased-momentum spacecraft due to its complex shape, optical properties and so on. In the case of spinning spacecraft, the working SRP is averaged due to high frequency spinning, so it is assumed that upper surface of spacecraft is roughly flat and SPR always radiates on the center of upper surface. However, in the case of biased-momentum spacecraft, which is not spinning, a deviation of irradiated surface and optical properties on each surface or component is generated. In this case, small, but important, additional torques are generated. Consequently, these additional SRP torque shifts the equilibrium point in a certain direction, which is depending entirely on the shape and optical properties of the spacecraft. This distorts the sun-tracking circular attitude motion.

3. Analytical Model of Sun-Tracking Motion

In this section, the sun-tracking motion of a biased-momentum 3-axis stabilized spacecraft under the influence of SRP is modeled analytically.

3.1. Definition and Assumption

In order to express spacecraft attitude, three coordinate frames are introduced; inertial frame Σ_I , orbit-fixed frame Σ_O and body-fixed frame Σ_B . The orthogonal basis system consists of vectors, \mathbf{i} , \mathbf{j} and \mathbf{k} . The subscript represents the attributed coordinate frame. The inertial frame is a frame of reference that is fixed in inertia space and time-independent. In the orbit-fixed frame, \mathbf{k}_O is always pointing to the sun direction, \mathbf{i}_O is pointing in the opposite direction of orbital motion and \mathbf{j}_O is perpendicular to the orbital plane. In the case of Hayabusa2, the body-fixed frame has \mathbf{i}_B pointing in the thruster injection direction, \mathbf{k}_B is the solar array panel (SAP) normal vector and \mathbf{j}_B is configured to form a right-hand system. (Fig.3 and Fig.4)

In the Hayabusa2 mission, the basic attitude of Hayabusa2 in cruising phase is almost sun-pointing so that the two fixed SAPs are facing the sun. By mounting one reaction wheel (RW) along the SAPs' normal vector \mathbf{k}_B , and generating angular momentum in that direction, sun-tracking motion is realized. In order to do so, it is assumed that the RW points exactly in the \mathbf{k}_B

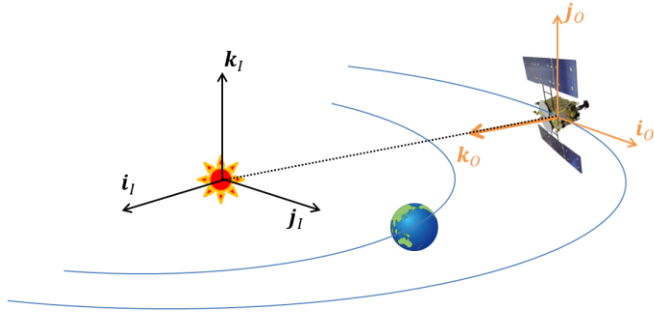


Figure 3. Orbit-fixed coordinate

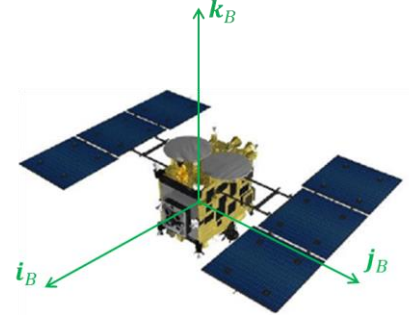


Figure 4. Body-fixed coordinate

direction and the inner angular momentum, which is described as \mathbf{h}_W , is also generated only in this direction.

The attitude of the body-fixed frame with respect to the orbit-fixed frame is represented as 2-1-3 ($\theta - \phi - \psi$) Euler expression, in modeling the attitude motion. In describing the spacecraft attitude, however, in-orbit angle β_{in} and out-orbit angle β_{out} are used to understanding where \mathbf{k}_B directs more easily. They are angles when spacecraft is looked at behind the sun. It is reasonable to consider that $\beta_{in} = \theta$ and $\beta_{out} = -\phi$. See Fig.5

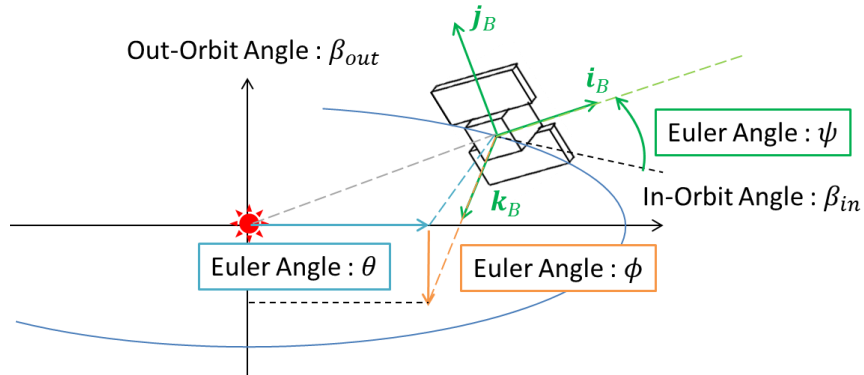


Figure 5. Euler angle expression and angles when looking at spacecraft behind the sun

In those definitions and assumptions, spacecraft-to-sun vector \mathbf{s} and inner angular momentum vector \mathbf{h}_W are respectively expressed, in the body-fixed frame, as below, where upper left superscript represents the coordinate frame which observes that vector:

$${}^B \mathbf{s} = \begin{pmatrix} -\sin\theta\cos\psi + \cos\theta\sin\phi\sin\psi \\ \sin\theta\sin\psi + \cos\theta\sin\phi\cos\psi \\ \cos\theta\cos\phi \end{pmatrix} \quad (2)$$

$${}^B \mathbf{h}_W = \begin{pmatrix} 0 \\ 0 \\ h_W \end{pmatrix} \quad (3)$$

Angular velocity vector of frame i with respect to frame j is represented in $\boldsymbol{\omega}_{i,j}$, so that of body-fixed frame to orbit-fixed and inertia frame, and that of orbit-fixed frame to inertia frame are respectively:

$${}^B \boldsymbol{\omega}_{B,O} = \begin{pmatrix} \omega_x \\ \omega_y \\ \omega_z \end{pmatrix}, \quad {}^O \boldsymbol{\omega}_{O,I} = \begin{pmatrix} 0 \\ \omega_0 \\ 0 \end{pmatrix} \quad (4)$$

$$\boldsymbol{\omega}_{B,I} = \boldsymbol{\omega}_{B,O} + \boldsymbol{\omega}_{O,I} \quad (5)$$

where ω_0 is orbital angular velocity decided by orbital radius.

In the case of 2-1-3 Euler angle expression, if angular velocity vector $\boldsymbol{\omega}_{B,O}$ is given, the following differential equation for the spacecraft's attitude angles with respect to orbit-fixed frame can be derived from rotation kinematics[8]:

$$\begin{pmatrix} \dot{\phi} \\ \dot{\theta} \\ \dot{\psi} \end{pmatrix} = \begin{pmatrix} \cos\psi & -\sin\psi & 0 \\ \sin\psi/\cos\phi & \cos\psi/\cos\phi & 0 \\ \sin\psi\tan\phi & \cos\psi\tan\phi & 1 \end{pmatrix} \begin{pmatrix} \omega_x \\ \omega_y \\ \omega_z \end{pmatrix} \quad (6)$$

3.2. One Wheel Control

In Hayabusa2 mission, sun-tracking motion is used in order to save fuel consumption and increase redundancy. As the attitude control actuator, four RWs are mounted on spacecraft in X-Y-Z1-Z2 arrangement, as is Fig. 6, which is very unique configuration. However, spacecraft uses only one RW along vector \mathbf{k}_B and the other three RWs are not operated. This control mode is called, one wheel control (OWC) mode. The only active RW is driven utilizing exactly the same control logic as is used by the ordinary three-axis stabilization controller to hold the attitude about vector \mathbf{k}_B , and it realizes sun-tracking motion. The other axes, \mathbf{i}_B and \mathbf{j}_B are passively maintained taking advantage of sun-tracking motion. During OWC mode, rotation angle around \mathbf{k}_B , which is ψ , is maintained constant with only one active RW control. So in this study, it is assumed that rotation angle ψ is always controlled constant.

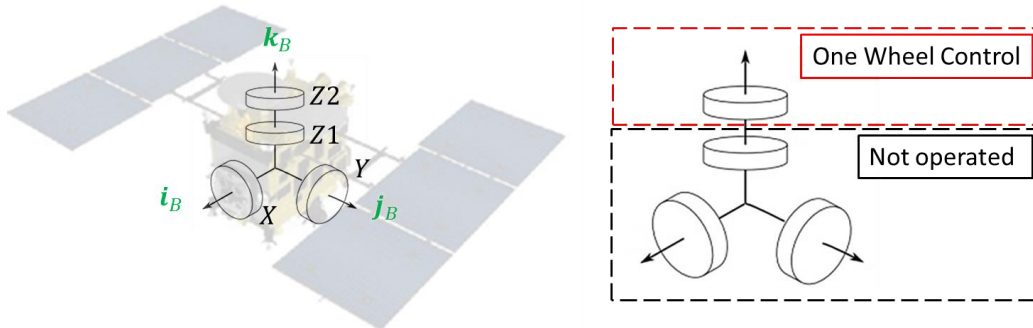


Figure 6. Four RW configuration and OWC mode

3.3. Solar Radiation Pressure Torque

In this section, analytical model of SRP torque working on biased-momentum 3-axis stabilized spacecraft is derived. SRP force working on every small radiated surface dA is expressed as:

$$d\mathbf{F}_{SRP} = -P \cdot dA(\mathbf{n} \cdot \mathbf{s}) \left\{ \left(2(\mathbf{n} \cdot \mathbf{s})C_s + \frac{2}{3}C_d \right) \mathbf{n} + (C_a + C_d)\mathbf{s} \right\} \quad (7)$$

where P is momentum flux, which is the energy carried by sunlight divided by the speed of light, \mathbf{n} is normal vector of small radiated surface and C_s, C_d and C_a are, respectively, the specular, diffusion and absorption constants of that surface. Then, SRP torque produced by such small radiated surface is:

$$d\mathbf{T}_{SRP} = \mathbf{l}_{SRP} \times d\mathbf{F}_{SRP} \quad (8)$$

$${}^B\mathbf{l}_{SRP} = \begin{pmatrix} x_{SRP} \\ y_{SRP} \\ z_{SRP} \end{pmatrix} \quad (9)$$

where \mathbf{l}_{SRP} is the vector from center of mass to radiated small surface. Then, SRP torque working on spacecraft is decided from integration in the total radiated area:

$$\mathbf{T}_{SRP} = \int_A d\mathbf{T}_{SRP} dA = \int_A \mathbf{l}_{SRP} \times d\mathbf{F}_{SRP} dA \quad (10)$$

During OWC mode, spacecraft is supposed to be always pointing to the sun direction roughly, so attitude angle ϕ and θ is assumed sufficiently small. Therefore, small angle approximation is adopted and following relationships hold true:

$$\sin\varphi \simeq \varphi, \cos\varphi \simeq 1 \quad (\varphi = \theta, \phi) \quad (11)$$

In such assumptions, it is revealed that SRP torque working on spacecraft is expressed using 9 parameters as below:

$${}^B\mathbf{T}_{SRP} = \begin{pmatrix} T_x \\ T_y \\ T_z \end{pmatrix}, \quad \begin{aligned} T_x &= D(\theta\cos\psi - \phi\sin\psi) - E(\theta\sin\psi + \phi\cos\psi) + F \\ T_y &= G(\theta\cos\psi - \phi\sin\psi) - H(\theta\sin\psi + \phi\cos\psi) + I \\ T_z &= J(\theta\cos\psi - \phi\sin\psi) - K(\theta\sin\psi + \phi\cos\psi) + L \end{aligned} \quad (12)$$

These 9 parameters are related to spacecraft shape and optical constants. Describing SAPs' normal vector \mathbf{n} and virtual center of SRP \mathbf{L}_{SRP} , which is the vector from center of mass to the averaged center point of all radiated surface, as:

$${}^B\mathbf{n} = \begin{pmatrix} n_x \\ n_y \\ n_z \end{pmatrix}, \quad {}^B\mathbf{L}_{SRP} = \begin{pmatrix} L_x \\ L_y \\ L_z \end{pmatrix} \quad (13)$$

these 9 parameters are approximately represented as:

$$\begin{aligned}
D &= P \left\{ \left(4C_s + \frac{5}{3}C_d + C_a \right) \int_A n_x y_{SRP} dA \right\} \\
E &= P \left\{ \left(4C_s + \frac{5}{3}C_d + C_a \right) \int_A n_y y_{SRP} dA - (C_a + C_d)L_z A \right\} \\
F &= P \left\{ \left(2C_s + \frac{2}{3}C_d \right) \int_A n_y z_{SRP} dA - \left(2C_s + \frac{5}{3}C_d + C_a \right) L_y A \right\} \\
G &= P \left\{ - \left(4C_s + \frac{5}{3}C_d + C_a \right) \int_A n_x x_{SRP} dA + (C_a + C_d)L_z A \right\} \\
H &= -P \left\{ \left(4C_s + \frac{5}{3}C_d + C_a \right) \int_A n_y x_{SRP} dA \right\} \\
I &= P \left\{ - \left(2C_s + \frac{2}{3}C_d \right) \int_A n_x z_{SRP} dA + \left(2C_s + \frac{5}{3}C_d + C_a \right) L_x A \right\} \\
J &= -P(C_a + C_d)L_y A \\
K &= P(C_a + C_d)L_x A \\
L &= P \left(2C_s + \frac{2}{3}C_d \right) \int_A r \left(\frac{\partial z_{SRP}}{r \partial \varphi} \right) dA
\end{aligned} \tag{14}$$

where r is the distance to a small radiated surface and φ is a phase angle around the \mathbf{k}_B .

Relationships between 9 parameters and spacecraft shape are described using simple solar sail model in Fig.7. By using simple solar sail model, it is easy to understand the characteristics of shape. In such a symmetry model, virtual center of SRP is approximated just the center point of spacecraft upper surface.

3.4. Attitude Model of Sun-Tracking Motion

In the case that there is no other disturbance except SRP, Euler equation Eq.1 is rewritten as:

$$\left. \frac{d\mathbf{H}}{dt} \right|_I = \left. \frac{d\mathbf{H}}{dt} \right|_B + \boldsymbol{\omega}_{B,I} \times \mathbf{H} = \mathbf{T}_{SRP} \tag{15}$$

$$\mathbf{H} = \mathbf{I} \cdot \boldsymbol{\omega}_{B,I} + \mathbf{h}_W \tag{16}$$

where the moment inertia is tensor \mathbf{I} , total angular momentum vector \mathbf{H} is the sum of that of attitude motion, which is $\mathbf{I} \cdot \boldsymbol{\omega}_{B,I}$, and inner angular momentum vector \mathbf{h}_W . For linearization, small angle approximation is adopted and the moment inertia tensor is approximated as:

$${}^B \mathbf{I} = \begin{pmatrix} I_x & 0 & 0 \\ 0 & I_y & 0 \\ 0 & 0 & I_z \end{pmatrix} \tag{17}$$

Substituting Eq.5, 6, 12, 16 and 17 into Eq.15, the equations of attitude motion in linearized form is obtained as:

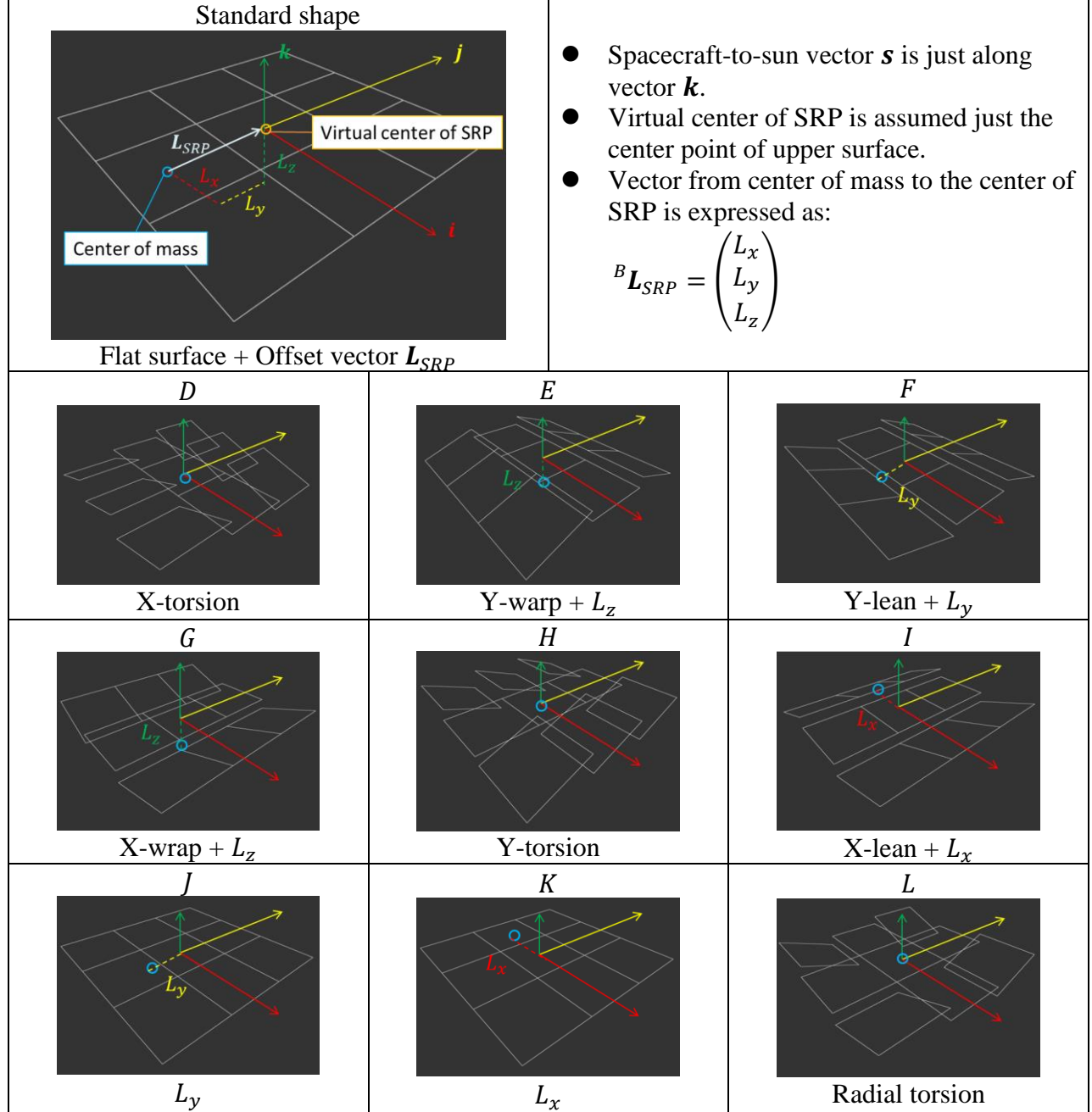


Figure 7. Relationships between 9 parameters and spacecraft shape

$$\begin{aligned}
 I_x(\ddot{\phi}\cos\psi + \ddot{\theta}\sin\psi) - h_w\{\dot{\phi}\sin\psi - (\dot{\theta} + \omega_0)\cos\psi\} \\
 &= D(\theta\cos\psi - \phi\sin\psi) - E(\theta\sin\psi + \phi\cos\psi) + F \\
 I_y(\ddot{\theta}\cos\psi - \ddot{\phi}\sin\psi) - h_w\{\dot{\phi}\cos\psi + (\dot{\theta} + \omega_0)\sin\psi\} \\
 &= G(\theta\cos\psi - \phi\sin\psi) - H(\theta\sin\psi + \phi\cos\psi) + I \\
 \dot{h}_w &= J(\theta\cos\psi - \phi\sin\psi) - K(\theta\sin\psi + \phi\cos\psi) + L
 \end{aligned} \tag{18}$$

where rotational angle ψ is kept constant due to OWC mode. These equations are linear and solved analytically.

In the case of Hayabusa2 it is reasonable to assume that $|E|, |G| \gg |D|, |H|$, E is negative and G is positive, because the shape of Hayabusa2 is roughly symmetric with respect to \mathbf{i}_B and \mathbf{j}_B , so that L_x, L_y are sufficiently small and L_z is much larger than them. In addition, the right side of third equation of Eq.18 is sufficiently small, so that in deriving analytical model, inner angular momentum h_W is assumed constant. Under these assumptions, sun-tracking motion is modeled analytically. That motion is divided into two parts; one is the motion of equilibrium point that is hardly moves, the other is the small motion around that equilibrium point. They are described as $\theta = \tilde{\theta} + \Delta\theta, \phi = \tilde{\phi} + \Delta\phi$, and each part is:

$$\begin{aligned} & \text{Equilibrium point} \\ \tilde{\theta} &= \frac{h_W \omega_0 \{H \cos^2 \psi + (E + G) \sin \psi \cos \psi + D \sin^2 \psi\} + IE \cos \psi - FG \sin \psi}{-GE} \\ \tilde{\phi} &= \frac{h_W \omega_0 \{G \cos^2 \psi + (D - H) \sin \psi \cos \psi - E \sin^2 \psi\} - FG \cos \psi - IE \sin \psi}{-GE} \end{aligned} \quad (19)$$

$$\begin{aligned} & \text{Attitude motion around equilibrium point} \\ \Delta\theta &= A_p \exp\left(\frac{D + H}{2h_W} t\right) \sqrt{-\frac{E}{G}} \left\{ \frac{\sqrt{-EG}}{h_W} t - \tan^{-1}\left(\frac{D + H}{\sqrt{-4EG}}\right) + \delta_p \right\} \\ \Delta\phi &= A_p \exp\left(\frac{D + H}{2h_W} t\right) \left\{ \frac{\sqrt{-EG}}{h_W} t + \delta_p \right\} \end{aligned} \quad (20)$$

where A_p, δ_p are integral constants and decided by initial condition. In sun-tracking motion of biased-momentum 3-axis stabilized spacecraft, there are three important and unique features, and they are confirmed from SRP torque vector field, as Fig. 8. In these figures, SRP torque vectors observed from orbit-fixed frame, which starting point is spacecraft's pointing direction and the length is torque absolute value if spacecraft directs to that point, are described.

1. Attitude motion around equilibrium point will converge or diverge due to $D + H$. If $D + H$ is positive, SRP torque vector field always directs outward and attitude motion will diverge and go away from equilibrium point. In the other hand, if $D + H$ is negative, SRP torque vector field always directs inward and attitude motion will converge and finally track to the exact equilibrium point.
2. Attitude motion around equilibrium point may be elliptic due to $\sqrt{-E/G}$. If $|E| > |G|$, SRP torque field draws elliptic circle, which is distorted in the in-orbit direction and attitude motion is also supposed to be elliptic and expanded in the in-orbit direction. If $|E| < |G|$, SRP torque field draws out-orbit direction distorted elliptic circle.
3. There is a phase difference of $\tan^{-1}\left((D + H)/\sqrt{-4EG}\right)$. In the case of Hayabusa2, $|E|, |G| \gg |D|, |H|$ is completed due to large L_z , a phase difference is considered to be nearly zero.

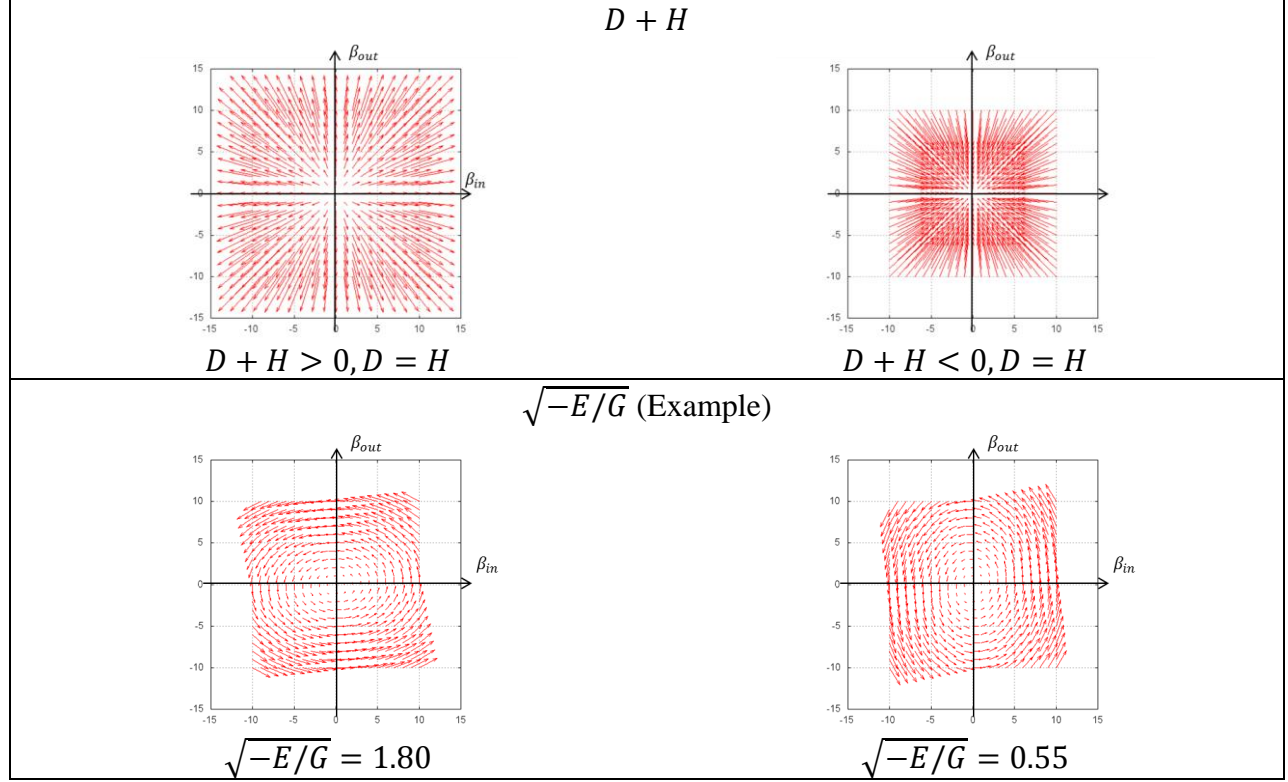


Figure 8. SRP torque vector field in the case of $\psi = 0$

4. Flight Data and Numerical Simulation

In this section, it is confirmed from flight data that Hayabusa2 really reproduced sun-tracking motion, and 9 parameter values are decided from it. Then, numerical simulation using such parameter values is compared with real one in order to check that analytical model is reasonable.

4.1. Flight Data of Hayabusa2

Figure 9 shows the flight data of Hayabusa2 during OWC mode, in this period rotational angle ψ was kept about 90[deg], from 9th to 20th February, 2015. The red line is the attitude history of \mathbf{k}_B , which is the combination motion of precession and nutation, and the green line is precession history extracted by averaging the red line every nutation cycle, which is just sun-tracking motion. As you can see, the equilibrium point is about $\beta_{in} = 1.2[\text{deg}]$, $\beta_{out} = 2.7[\text{deg}]$, and attitude motion around that point is distorted in the out-orbit direction and seems to diverge a little bit. 9 parameter values are decided from flight data using least-squares method as Tab.1.

4.2. Numerical Simulation

Numerical simulation, which is time integration of Eq.15 using parameter values decided from flight data in that right side, is described in Fig.10. Initial and calculation condition is shown in Tab.2. This results, both attitude motion and inner angular momentum, agree well with the real flight data. Therefore, this analytical model is reasonable to predict attitude motion of Hayabusa2 for future mission period.

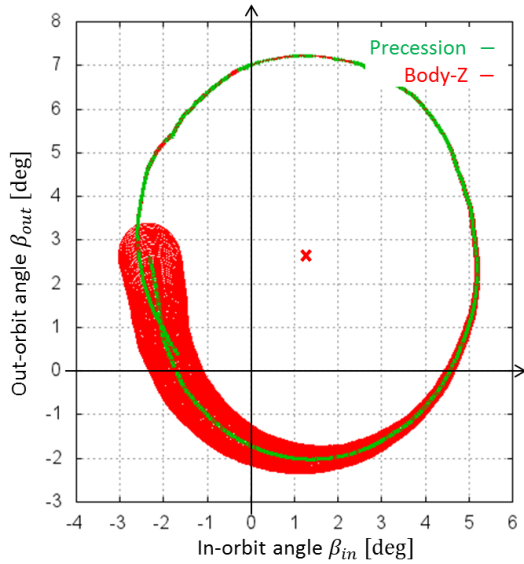


Table 1. Parameter values from flight data

D	3.97×10^{-7}
E	-2.37×10^{-5}
F	-5.68×10^{-7}
G	1.71×10^{-5}
H	-1.51×10^{-7}
I	-1.25×10^{-6}
J	3.44×10^{-6}
K	-4.34×10^{-9}
L	-2.33×10^{-7}

Figure 9. Flight data of Hayabusa2 Feb. 9th-20th, 2015, $\psi = 90$ [deg]

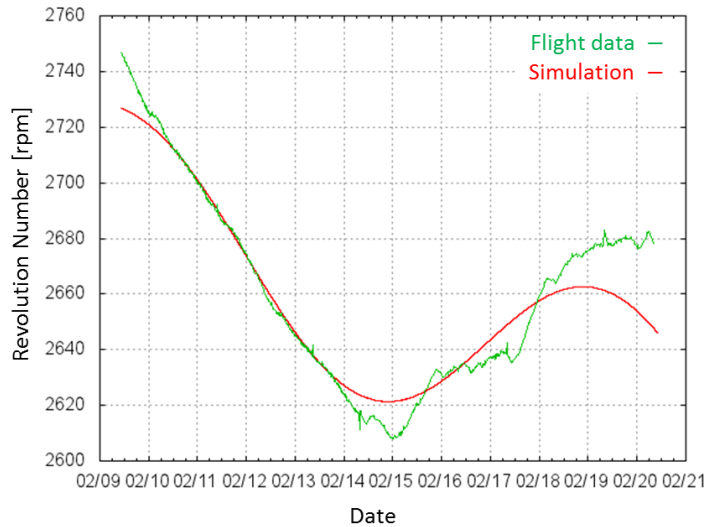
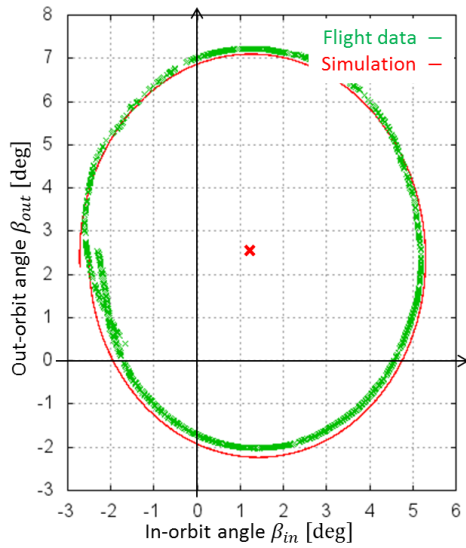


Figure 10. Comparison of simulation result with flight data

5. Conclusion

The attitude motion of biased-momentum 3-axis stabilized spacecraft is modeled, and it is expressed in 9 parameters. These 9 parameters are largely related with the shape of spacecraft and optical constants of each component. It is revealed that only in the case of biased-momentum 3-axis stabilized spacecraft, the equilibrium point has offset not only in the out-orbit direction, but also in the in-orbit direction, furthermore, the attitude motion around that equilibrium point may be ellipse which would converge or diverge. This analytical model is confirmed from the real flight data of Hayabusa2. Using this model, it is possible to predict the attitude motion of

Table 2. Initial and calculation condition

Initial condition					
$\beta_{in} = \theta$ [deg]	$\beta_{out} = -\phi$ [deg]	ψ [deg]	h_W [Nms]	$\omega_{B,0}$ [deg/sec]	
-2.5	-2.5	90.0	3.0	0.0	
Calculation condition					
Solar distance [AU]					
1.073					
Moment of Inertia [kg · m ²]					
I_{xx}	I_{yy}	I_{zz}	I_{xy}	I_{yz}	I_{zx}
381.27	315.81	469.04	-3.25	0.76	8.65

Hayabusa2 for future mission period. This is the generalized model of attitude motion under the large influence of SRP, so it is possible to apply this model for any other shape spacecraft in the future.

6. Acknowledgments

This work was supported by Japan Society for the Promotion of Science Grant-in-Aid for Scientific Research, 26289325.

7. References

- [1] Nishida, S. "Recent Trends in Three-Axis Stabilized Satellites." Journal of the Japan Society for Aeronautical and Space Sciences, Vol. 22, No. 243, pp. 200-207, 1974
- [2] Kawaguchi, J. and Shirakawa, K. "A Fuel-Free Sun-Tracking Attitude Control Strategy and the Flight Results in Hayabusa (MUSES-C)" Proceedings of the AAS/AIAA Space Flight Mechanics Meeting, 2007
- [3] Kominato, T., Shirakawa, K., Matsuoka, M., Uratani, C. and Oshima T. "Hayabusa Attitude Control for delta-V Operations." Proceedings of Workshop on JAXA Astrodynamics and Flight Mechanics, 2007
- [4] Funase, R., Mimasu, Y., Shirasawa, Y., Tsuda, Y., Saiki, T., Kawaguchi, J. and Chishiki, Y. "Modeling and On-Orbit Performance Evaluation of Propellant-Free Attitude Control System for Spinning Solar Sail via Optical Parameter Switching" Proceeding of the AAS/AIAA Astrodynamics Specialist Conference, 2012
- [5] Funase, R., Shirasawa, Y., Mimasu, Y., Mori, O., Tsuda, Y., Saiki, T. and Kawaguchi, J. "On-Orbit Verification of Fuel-Free Attitude Control System for Spinning Solar Sail Utilizing Solar Radiation Pressure" Advances in Space Research, Vol. 48, No. 11, 2011
- [6] Tsuda, Y., Yoshikawa, M., Abe, M., Minamino, H. and Nakazawa, S. "System Design of The Hayabusa2 – Asteroid Sample Return Mission To 1999 JU3" ActaAstronautica, Vol. 90, pp. 356-362, doi: 10.1016/j.actaastro.2013.06.028, 2013

[7] Tsuda, Y., Ono, G., Akatsuka, K., Saiki, T., Mimasu, Y., Ogawa, N. and Terui, F. "Generalized Attitude Model for Momentum-Biased Solar Sail Spacecraft" (Preprint) AAS

[8] Wertz, J.R. Ed. "Spacecraft Attitude Determination and Control" Kluwer Academic Publishers, Boston, pp. 765-766, 1978